Chinese Journal of Chemistry
中国化学 - An International Journal

Accepted Article

Title: Design, Synthesis and SAR Studies of Novel and Potent Dipeptidyl Peptidase 4 Inhibitors

Authors: Na Luo, Xiaoyu Fang, Mingbo Su, Xinwen Zhang, Dan Li, Honglin Li, Shiliang Li* and Zhenjiang Zhao*

This manuscript has been accepted and appears as an Accepted Article online.

This work may now be cited as: *Chin. J. Chem.* **2020**, *38,* 10.1002/cjoc.202000342.

The final Version of Record (VoR) of it with formal page numbers will soon be published online in Early View: http://dx.doi.org/10.1002/cjoc.202000342.

WILEY-VCH SIOC CCS

ISSN 1001-604X • CN 31-1547/O6
mc.manuscriptcentral.com/cjoc
www.cjc.wiley-vch.de

CJC Chinese Journal of Chemistry
中国化学 - An International Journal

Accepted Article

Title: Design, Synthesis and SAR Studies of Novel and Potent Dipeptidyl Peptidase 4 Inhibitors

Authors: Na Luo, Xiaoyu Fang, Mingbo Su, Xinwen Zhang, Dan Li, Honglin Li, Shiliang Li* and Zhenjiang Zhao*

This work may now be cited as: *Chin. J. Chem.* **2020**, *38,* 10.1002/cjoc.202000342.

The final Version of Record (VoR) of it with formal page numbers will soon be published online in Early View: http://dx.doi.org/10.1002/cjoc.202000342.

WILEY-VCH SIOC CCS

ISSN 1001-604X • CN 31-1547/O6
mc.manuscriptcentral.com/cjoc
www.cjc.wiley-vch.de

Report

Type II diabetes; Dipeptidyl peptidase IV; Inhibitors; Molecular docking; Structure-activity relationship

CJC Chinese Journal of Chemistry 中国化学 - An International Journal

Design, Synthesis and SAR Studies of Novel and Potent Dipeptidyl Peptidase 4 Inhibitors

Na Luo,[a] Xiaoyu Fang,[a] Mingbo Su,[b] Xinwen Zhang,[b] Dan Li,[c] Honglin Li[a], Shiliang Li*,[a] and Zhenjiang Zhao *,[a]

[a]Shanghai Key Laboratory of New Drug Design, School of Pharmacy, East China University of Science and Technology, 130 Meilong Road, Shanghai 200237, China
[b]State Key Laboratory of Drug Research, Shanghai Institute of Materia Medica, Chinese Academy of Sciences. 555 Zhuchongzhi Raad Shanghai 201203, China
[c]Shangdong Biopolar Dichang Pharmaceutical Co.,Ltd. RM2306, No.786 Linzi Avenue, Zibo, Shangdong, 255400, China

Cite this paper: *Chin. J. Chem.* ***2019****, 37, XXX—XXX.* ***DOI: 10.1002/cjoc.201900XXX***

Summary of main observation and conclusion Dipeptidyl Peptidase 4 (DPP-4) is a clinically validated target for the treatment of type 2 diabetes mellitus (T2DM). To discover novel and potent DPP-4 inhibitors, three series of compounds were designed and synthesized in this study based on our previously identified novel scaffold of 2-phenyl-3,4-dihydro-2*H*-benzo[*f*]chromen-3-amine. Among the designed compounds, **41d-1** was the most potent one with an IC_{50} value of 16.00 nM. Besides, **41d-1** (5 mg/kg) displayed a moderate glucose tolerance capability in ICR mice. Structure-activity-relationship (SAR) studies were discussed in detail, which is constructive for our further optimization.

Background and Originality Content

Diabetes is a severe chronic metabolic disorder. According to the newest data of IDF, there are about 463 million people in adults with diabetes around the world. The prevalence of diabetes is expected to reach 700 million by 2045 and puts a huge burden on the health-care system. T2DM accounts for around 90% of cases of diabetes.[1] T2DM could lead to microvascular (stroke, myocardial infarction) and macrovascular complications (neuropathy, nephropathy) that cause profound psychological and physical distress to both patients and carers.[2-3] Traditional oral antidiabetic agents including biguanides, sulfonylureas, thiazolidinediones, glinides, α-glucosidase inhibitors helped patients a lot, but these agents have been associated with undesirable side effects such as hypoglycemia, weight gain and gastrointestinal reactions.[4] To explore new, safe and effective approaches for T2DM therapy, several antidiabetic drugs with new mechanisms including SGLT-2 inhibitors, GLP-1R agonists and DPP-4 inhibitors have been developed. DPP-4 inhibitors have been the most recently developed agents for the treatment of T2DM.[5] Up to now, 11 DPP-4 inhibitors have been marketed around the world, and some typical gliptins are shown in **Figure 1**.

DPP-4 is a ubiquitous serine protease that deactivates a variety of other bioactive peptides with alanine, proline or serine at the penultimate position of the N-terminus.[6] Incretins such as GLP-1 and GIP regulate postprandial blood glucose by a glucose-dependent manner and responsible for 50-70% insulin release.[7] These two incretins stimulate secretory of insulin in response to food ingestion by recognizing G protein-coupled receptors on pancreatic β cells [5]. GLP-1 could also decrease islet glucagon secretion, slow gastric emptying and increase satiety.[6, 8] However, endogenous GLP-1 has a short half-time of 1-2 minutes due to being recognized and degraded by DPP-4 enzymes.[8] Therefore, DPP-4 inhibitors play a vital role in preserving the function of GLP-1 and GIP, thus controlling the level of blood glucose and benefiting the β cell. Compared to traditional antihyperglycemic drugs, DPP-4 inhibitors have more advantages, including ease of administration, no weight gain and a low risk of hypoglycemia in clinical practice.[9-10]

In our previous work, starting with a natural scaffold of iso-daphnetin (compound **6**) and sitagliptin, a novel lead 2-phenyl-3,4-dihydro-2*H*-benzo[*f*]-chromen-3-amine (**8**) was designed utilizing pharmacophore grafting and scaffold hopping.[11] Further structural modification guided by fragment molecular orbital (FMO) method gave a promising candidate (**7, Figure 2**) with dramatic improvement in potency (IC_{50} = 2.10 nM). Further *in vivo* evaluation showed that **7** could inhibit >80% of DPP-4 activity for more than 7 days with a single oral dose of 3 mg/kg in diabetic mice. The long-term antidiabetic efficacies of **7** (10 mg/kg, qw) were better than those of the once-weekly omarigliptin (**3**) and trelagliptin (**4**).[12]

In this study, with the expectation of exploring more novel and active DPP-4 inhibitors, several modification strategies were conducted based on the dihydrobenzo[*f*]chromen core of **7**. First, we moved the tail phenyl ring of the naphthalene moiety from the [*f*] side to [*h*] side while kept the orientation of the substituents to the S2 extensive pocket (Val207, Arg357, Arg358, Ser209), then a new family of 2-(2,4,5-trifluorophenyl)-3,4-dihydro-2*H*-benzo[*h*]chromen-3-amine derivatives were designed. However, dihydrobenzo[*h*]chromen analogs displayed less potent than **8** due to steric clashes. In order to eliminate unfavorable clashes, a series of 2-(2,4,5-trifluorophenyl)-6-phenyl-3,4-dihydro-2*H*-chroman-3-amine derivatives were designed. Besides, based on the similar physicochemical properties between atoms O and S, we adopted bioisosterism strategy and a series of 2-(2,4,5-trifluorophenyl)-3,4-dihydro-2*H*-benzo[*f*]thiochromen-3-amine derivatives were designed. Herein, we reported the synthesis, SAR studies and biological evaluation of these three series of derivatives based on the novel skeletons (**Figure 3**).

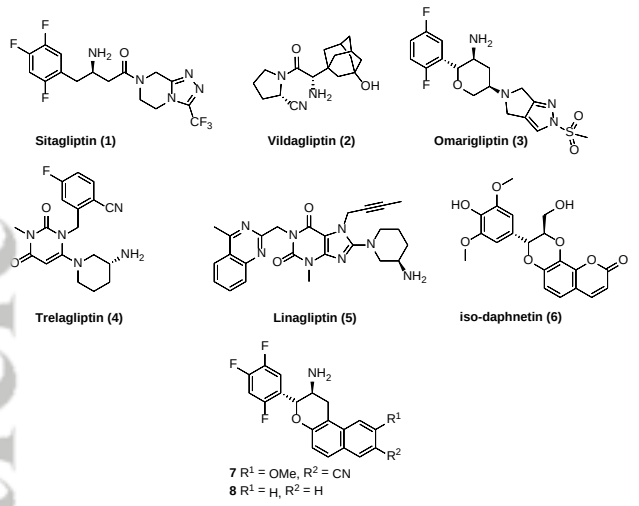

Figure 1 Representative DPP-4 inhibitors.

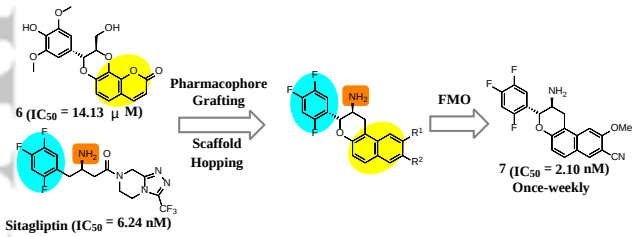

Figure 2 Our previous work

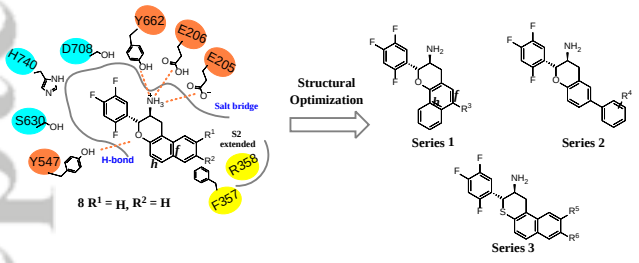

Figure 3 Design and modification strategies of novel DPP-4 inhibitors.

Results and Discussion

Synthesis

Scheme 1 mainly describes the general synthesis of **17a-j** and **22**. Compound **10** was obtained from the condensation of 2,4,5-triflfluorobenzaldehyde **9** and nitromethane. **11c** was given by esterification of reagent **11b** with MeOH and H_2SO_4. Then starting from **11d**, compounds **11e** and **11f** were prepared by similar substitution reactions with CH_3SO_2Cl and Tf_2O, respectively. **11g** and **11h** were afforded by Suzuki-Miyaura coupling of **11a** with respective boric esters. Naphthaldehyde **12a-f** could be prepared by formylation of corresponding starting materials **11a**, **11c**, **11e-h** in the presence of 1,1-dichlorodimethyl ether/$TiCl_4$, while **12g** was obtained by nucleophilic substitution of **12a** with morpholine. Then compounds **12a-g** could be converted to hydroxyl naphthaldehyde **14c-i** by demethylation in the presence of anhydrous $AlCl_3$, while **14a-b** were obtained by the same method as the synthesis of **12a** form **13a-b**. Intermediates **15a-i** were successfully obtained by Michael addition and aldol condensation of **14a-i** and compound **10**. Mixtures of *cis/trans* dihydrobenzo[*h*]chromen derivatives **16a-i** were given by reduction of **15a-i** with $NaBH_4$; configuration transformation of the *cis* isomers to the *trans* isomers could occur in one-pot upon exposure to N,N-Diisopropylethylamine (DIPEA).[13] Subsequently, **16a-i** were reduced with Zn powder to yield resulting dihydrobenzo[*h*]chromen amine **17a-i** via column chromatography isolation. Compound **17j** was produced by ester hydrolysis of **17d**. Starting from **18**, compound **19** was given by Vilsmeier-Haack reaction, and then compound **22** was provided by similar steps from **19** as preparation of **17a**.

Scheme 1 Synthesis of 2-phenyl-3,4-dihydro-2*H*-benzo[*h*]chromen-3-amine derivatives[a]

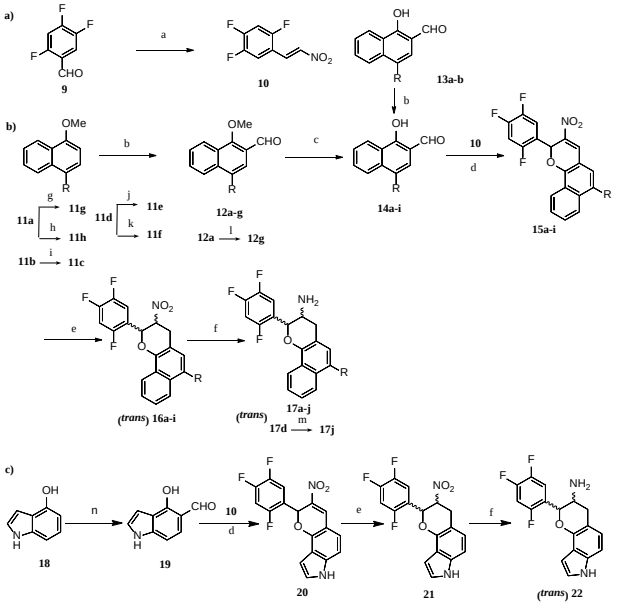

[a]Reagents and conditions: (a) CH_3NO_2, NaOH aq, CH_3OH, 0-5 °C; $ZnCl_2$ aq, con. HCl, 5-10 °C, 78% for two steps; (b) 1,1-dichlorodimethyl ether,$TiCl_4$, 0 °C to r.t., 22%-79%; (c) anhydrous $AlCl_3$, DCM, 0 °C to 40 °C, 40%-66%; (d) L-pipecolinic, Toluene, 120 °C, N_2, 10%-42%; (e) 1) $NaBH_4$, THF/CH_3OH, r.t.; 2) DIPEA, EtOH, r.t., 40%-55% for two steps; (f) Zn, HCl, EtOH, r.t., 10%-25%; (g) (3,6-dihydro-2H-pyran-4-yl)-boronic acid pinacol ester, $Pd(PPh_3)_4$, Cs_2CO_3, DMF/H_2O, 90 °C, N_2; (2) Pd/C, H_2, MeOH, r.t., 73% for two steps; (h) (3-(methylsulfonyl)phenyl)boronic acid, $Pd(PPh_3)_4$, Cs_2CO_3, DMF/H_2O, 95 °C, N_2, 73%; (i) CH_3OH, H_2SO_4, 70 °C, 95%; (j) CH_3SO_2Cl, pyridine, DCM, 0 °C to r.t., 45%; (k) Trifluoromethylsulfonic anhydride, Et_3N, DCM, -78 °C to r.t., 68%; (l) morpholine, $Pd_2(dba)_3$, BINAP, t-BuOK, Toluene,100 °C, N_2, 49%; (m)

NaOH, MeOH/H_2O, 50 °C, 50%; (n) $POCl_3$, DMF, 0 °C to r.t., 69%.

Scheme 2 describes the general synthesis of 2-(2,4,5-trifluorophenyl)-6-phenyl-3,4-dihydro-2*H*-chroman-3-amine derivatives. Salicylaldehyde analogs **28a-j** were given by Suzuki-Miyaura coupling of corresponding starting materials **27a-j** with 5-bromo-2-hydroxybenzaldehyde (**23**). Next, as described in **Scheme 1**, **29a-j** were synthesized by Michael addition and aldol condensation of **28a-j** and **10**. Subsequently, *trans* isomers **30a-j** were obtained by reduction of **29a-j** with $NaBH_4$ followed by configuration transformation. Finally, compounds **31a-j** were given by reduction of **30a-j** with Zn powder. Starting from **23**, compound **26** was given by similar steps like preparation of **31a-j**.

Scheme 2 Synthesis of 2-phenyl-6-phenyl-3,4-dihydro-2*H*-chroman-3-amine derivatives[a]

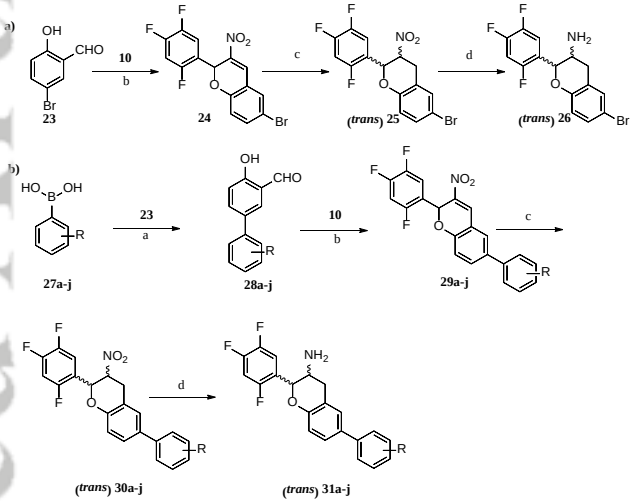

[a]Reagents and conditions: (a) Cs_2CO_3, $PdCl_2(dppf)_2$, DMF/H_2O, 100 °C, N_2, 31-51%; (b) L-pipecolinic, toluene, 120 °C, N_2, 23%-50%; (c) 1) $NaBH_4$, THF/CH_3OH, r.t.; 2) DIPEA, EtOH, r.t., 45%-55% for two steps; (d) Zn, HCl, EtOH, r.t., 20%-69%.

Scheme 3 lists the overall synthesis routine of dihydrobenzo[*f*]thiochromen amine derivatives. The 2-naphthaldehyde **33a-b** were prepared by formylation of starting materials **32a-b** in the presence of 1,1-dichlorodimethyl ether. Then **33a-b** were converted into **35a-b** by demethylation in the presence of $AlCl_3$, while **35c-f** were directly afforded by formylation of **34a-d** as the same method of the preparation of **33a-b**. Then thiophenol **38a-f** were prepared via Newman–Kwart rearrangement (NKR) from naphthol **35a-f** for three steps.[14] First, compounds **36a-f** were obtained by esterification of compounds **35a-f** and dimethylthiarbamoyl chloride in the presence of DABCO. Second, S-arylthioarbamate **37a-f** were obtained from O-arylthiocarbamate **36a-f** under microwave irradiation. Finally, **37a-f** were converted into **38a-f** via ester hydrolysis. Benzo[*f*]thiochromen analogs **39a-f** were given by **38a-f** in the presence of **10** via Michael addition and aldol condensation. Dihydrobenzo[*f*]thiochromen derivatives **40a-f** were given by $NaBH_4$ reduction and configuration transformation form **39a-f**. Dihydrobenzo[*f*]thiochromen amine derivatives **41a-f** were finally given by reduction of Zn and hydrochloric acid form **40a-f**, while **41g** was given by hydrolysis from **41d**. We also conducted chiral column chromatography of **41d** with high activity to get the single isomer.

Scheme 3 Synthesis of 2-phenyl-3,4-dihydro-2*H*-benzo[*f*]thiochromen-3-amine derivatives[a]

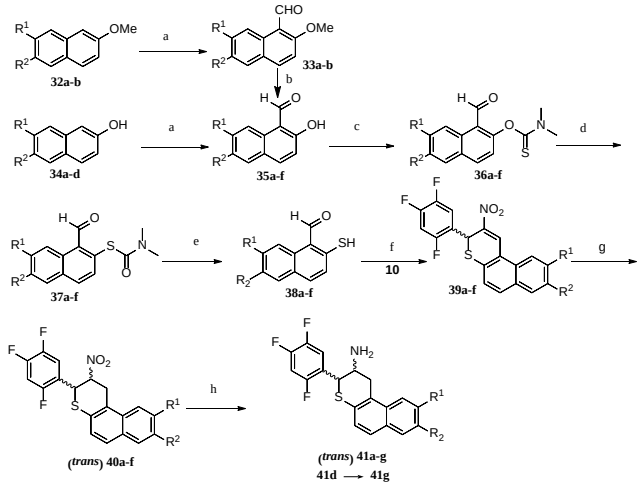

[a]Reagents and conditions: (a) 1,1-dichlorodimethyl ether, $TiCl_4$, DCM, 0 °C-r.t., 17%-46%; (b) anhydrous $AlCl_3$, DCM, 0-40 °C., 47%-93%; (c) dimethylthiarbamoyl chloride, DABCO, 0-50 °C, 59%; (d) MW, 200-230 °C, 150-200 W, 30%-45%; (e) 3N NaOH, CH_3OH, 65 °C; (f) 1,1,3,3-tetramethylguanidine, toluene, 80 °C, 12%-30%; (g) 1) $NaBH_4$, THF/CH_3OH, r.t.; 2) DIPEA, EtOH, r.t., 15%-30% for two steps; (h) Zn, 6N HCl, EtOH, r.t., 5%; (i) 45% H_2SO_4 aq., reflux, 20%; (j) chiral separation (Chiralpak ID 0.46 cm × 15 cm column; mobile phase MeOH/DEA = 100/0.1 (v/v); flow rate, 1.0 mL/min).

Structure-activity relationship

Compounds listed in **Tables 1-3** were evaluated *in vitro* for DPP-4 inhibition.

Table 1 Activities of 2-phenyl-3,4-dihydro-2*H*-benzo[*h*]chromen-3-amine derivatives against the DPP-4 enzyme.

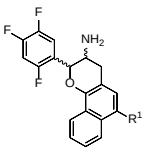

Compound[a]	R^1	IC_{50} (nM)[b]

8	-	110.10 ± 5.67
17a	H	1536.70 ± 30.41
17b	OMe	650.71 ± 13.20
17c	Br	5169.64 ± 285.23
17d	COOMe	288.04 ± 78.89
17e	$NHSO_2CH_3$	319.84 ± 34.01
17f	tetrahydropyrane	191.06 ± 44.45
17g	morpholine	197.75 ± 18.97
17h	Ph-3-Ms	782.02 ± 12.73
17i	$NHSO_2CF_3$	5226.23 ± 207.95
17j	COOH	3918.63 ± 149.73
22	-	993.71 ± 108.92
Omarigliptin	-	2.20 ± 0.66
Trelagliptin	-	2.58 ± 0.73

[a]Compounds are *trans*-racemic structures. [b]Mean values of at least three independent experiments.

Results of dihydrobenzo[*h*]chromen amine derivatives were shown in **Table 1**. Comparing **17a** with compound **8**, more than a 10-fold decrease in potency was observed. Considering that the distance between O atom of naphthalene and C atom of Tyr547 (3.1 Å) is shorter than the sum of van der Waals radius of the two atoms (3.22 Å), **17a** may have steric clashes with Tyr547, which may contribute to the great loss in potency (**Figure 4A**). When small groups like –OMe and –Br were introduced, opposite results were observed, which suggests that hydrophilic group (-OMe) is more favorable than the hydrophobic one (-Br) in the solvent area. Considering that there is a wide entrance of S2 extended pocket, other larger groups could be introduced to the R^1 position to occupy S2 extended pocket. Therefore, substituents like –COOMe, $–NHSO_2CH_3$, tetrahydropyrane and morpholine were introduced. These compounds displayed better potency as expected. Noticeably, comparing to **17a**, large heterocycle substituents like compounds **17f** (IC_{50} =191.06 nM) and **17g** (IC_{50} =197.75 nM) displayed around 8-fold boost in potency. The potency improvement of **17f** and **17g** suggests that shape matching is an important factor for improving activities. The predicted binding mode of **17f** showed that hydrogen bond interaction could be formed between the oxygen atom of the tetrahydropyrane group and the hydroxyl of Ser209 (**Figure 4B**). However, bulky groups like Ph-3-Ms of **17h** (IC_{50} =782.02 nM) offered no advantage over **17f**. We speculated that the binding affinity of **17h** might be weakened by the unfavorable intramolecular tension introduced by the two H atoms of naphthalene ring and the substituted phenyl group. Strong polar groups such as –COOH, $-NHSO_2CF_3$ displayed a dramatic reduction of potencies. Moreover, compound **22**, an indole analog, was designed to eliminate the steric clashes mentioned above in dihydrobenzo[*h*]chromen amine analogs. As a result, **22** performed better than **17a** as expect.

In a further modification, naphthalene fragment was replaced by the biphenyl group to eliminate the unfavorable intermolecular collision aforementioned, then a series of 2-(2,4,5-trifluorophenyl)-6-phenyl-3,4-dihydro-2*H*-chroman-3-amine derivatives were synthesized and evaluated.

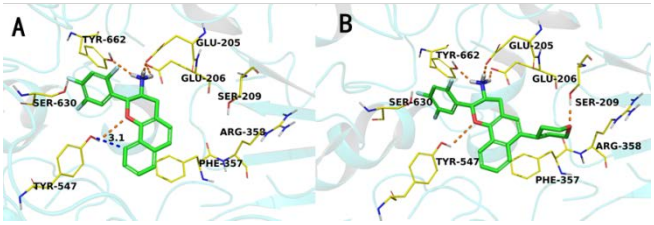

Figure 4 Predicted binding modes of **17a** (**A**) and **17f** (**B**). The structure of DPP-4 is shown in a light blue cartoon (PDB id: 4PNZ), the key residues are displayed as thin yellow sticks, **17a** and **17f** are shown as thick green sticks, hydrogen bonds are displayed as orange dashed lines, atom-atom distance is marked as blue dashed lines.

Compounds based on the biphenyl fragment are shown in **Table 2**. First, compound **31a** was synthesized and performed better in potency than **17a**. When replacing the phenyl group with –Br, a slight improvement in potency was observed. In order to further improve the potency, we decided to introduce some larger substituents onto the phenyl group of **31a**. As displayed in **Table 2**, substituents on the 3-position could bring enhanced potency. Compounds **31b-e** with hydrogen-bond receptors were more potent than **31a**, especially compound **31b** (IC_{50} = 112.22 nM), which is connected with $3\text{-}SO_2CH_3$, displayed over 10-fold improvement in potency. Moreover, given the strong positive electrostatic potential of the S2 extended pocket, some electron-withdrawing groups like –CN, -COOH and tetrazole were introduced. Just as expected, compounds **31f-h** were more potent than **31a**. **31g** with a tetrazole group displayed the best *in vitro* potency (IC_{50} = 98.74 nM) among the biphenyl-based compounds. Compounds **31i** and **31j** with di-substituted groups also performed better than **31a**. **31j** (IC_{50} = 409.26 nM) with 3,4-dimethoxy substituent was more potent than **31i**, which may due to the strong negative electrostatic potential produced by the

co-occurrence of the two methoxy oxygen atoms.[12] The predicted binding mode of **31g** showed that charge-reinforced hydrogen bond interaction could be formed between the tetrazole group and Arg358 (**Figure 5**). Potency improvement of **31g** suggests that electrostatic complementarity is an important factor for our further optimization.

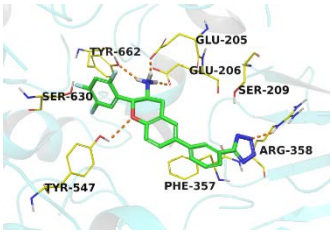

Figure 5 Predicted binding mode of **31g**. The structure of DPP-4 is shown in a light blue cartoon (PDB id: 4PNZ), the key residues are displayed as thin yellow sticks, **31g** is represented as thick green sticks, hydrogen bonds are displayed as orange dashed lines.

Table 2 2-phenyl-6-phenyl-3,4-dihydro-2*H*-chroman-3-amine derivatives against the DPP-4 enzyme.

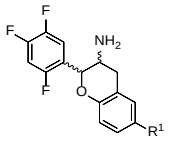

Compound[a]	R^1	IC_{50} (nM)[b]
26	Br	1202.83 ± 159.65
31a	Ph	1360.71 ± 478.49
31b	Ph-3-Ms	112.22 ± 12.08
31c	Ph-3-COOMe	622.34 ± 141.89
31d	Ph-3-$NHSO_2CH_3$	274.49 ± 77.84
31e	Ph-3-$NHSO_2CF_3$	841.70 ± 202.52
31f	Ph-3-COOH	140.51 ± 29.52
31g	Ph-3-tetrazole	98.74 ± 22.19
31h	Ph-3-CN	348.06 ± 84.64
31i	Ph-2,4-DiF	746.61 ± 128.01
31j	Ph-3,4-DiOMe	409.26 ± 206.95
Omarigliptin	-	2.20 ± 0.66
Trelaglitpin	-	2.58 ± 0.73

[a]Compounds are *trans*-racemic structures. [b]Mean values of at least three independent experiments.

Results of dihydrobenzo[*f*]thiochromen analogs were summarized in **Table 3**. When replacing the O atom by S atom, the potency increase in compound **41a** was observed, which may benefit from the favorable van der Waals interactions between **41a** and the active site of DPP-4. In order to explore more potent compounds, different substituents were introduced to R^1 and R^2 positions of **41a**. For the R^1 position, both **41c** and **41e** performed weaker potency than **41a**, suggesting that substituents in the R^1 position were unfavorable to potency improvement. While for the R^2 position, polar groups such as –CN (**41d**) and –COOH (**41g**) brought increases in activities comparing with **41b** containing a –Br group. Similarly, incorporating a polar cyano group at the R^2 position of **41e**, potency improvement was also observed (**41f**). Based on the exploration of R^2 position, we can conclude that polar groups are beneficial to improving potency. **41d** was the most active compound and separated as (2R,3S)-isomer (**41d-1**) with an IC_{50} value of 16.00 nM. The binding mode of the **41d-1** suggests that the 2,4,5-trifluorobenzene group penetrates into the hydrophobic subpocket of DPP-4 formed by residues Val656, Tyr631, Tyr662, Trp659, Tyr666, and Val711, while the tetrahydro-2*H*-thiopyran-3-amine nitrogen atom positions appropriately to generate salt-bridge and hydrogen bond interactions with the side chains of Glu205, Glu206, and Tyr662. The naphthalene fragment forms π-π stacking interactions with Phe357. Besides, the electron-withdrawing –CN could form a charge-reinforced hydrogen bond with the flexible Arg358 (**Figure 6**).

Table 3 Activities of 2-Phenyl-3,4-dihydro-2*H*-Benzo[*f*]thiochromen-3-amine Derivatives against the DPP-4 enzyme.

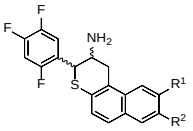

Compound[a]	R^1	R^2	IC_{50} (nM)[b]
41a	H	H	33.27 ± 14.15
41b	H	Br	253.43 ± 6.69
41c	Br	H	151.04 ± 55.43
41d	H	CN	21.44 ± 5.23
41d-1	H	CN	16.00 ± 2.11
41d-2	H	CN	400.99 ± 52.35
41e	OMe	H	125.44 ± 14.25
41f	OMe	CN	86.76 ± 33.42
41g	H	COOH	121.62 ±22.52
Omarigliptin	-	-	2.20 ± 0.66
Trelagliptin	-	-	2.58 ± 0.73

[a]The absolute configuration of **41d-1** is (*2R,3S*), the absolute configuration of **41d-2** is (*2S,3R*). The other compounds are *trans*-racemic structures. [b]Mean values of at least three independent experiments.

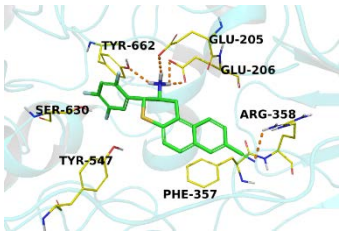

Figure 6 Predicted binding mode of **41d-1**. The structure of DPP-4 is shown in a light blue cartoon (PDB id: 5J3J), the key residues are displayed as thin yellow sticks, **41d-1** is represented as thick green sticks, hydrogen bonds are displayed as orange dashed lines.

Oral glucose tolerance test (OGTT) in ICR mice

Considering the good in vitro potency of compound **41d-1** against DPP-4, we further conducted an OGTT to preliminarily evaluate its ability of improving the glucose clearance capacity in vivo. The results showed that **41d-1** displayed a moderate blood glucose reduction efficacy at a low dosage of 5 mg/kg by decreasing the $AUC_{0-120min}$ of 4.38% (**Table S1** and **Figure S1** in supporting information). Higher dosages will be explored in our future study to comprehensively evaluate the in vivo anti-diabetic efficacy of **41d-1**.

Conclusions

In summary, aiming to discover novel DPP-4 inhibitors with high potency, structural modifications were conducted based on the skeleton of our preclinical candidate **7**. Three new series of potent DPP-4 inhibitors with the scaffolds of dihydrobenzo[*h*]chromen, biphenyl and dihydrobenzo[*f*]thiochromen were synthesized and evaluated. Their SAR was studied and discussed. Dihydrobenzo[*h*]chromen analogs displayed moderate activities that may attribute to the unfavorable steric clashes between the ligands and protein. Potency improvement of **31g** based on the biphenyl skeleton suggested that electrostatic complementarity should be taken into consideration in future structural optimization. Among the derivatives explored, **41d-1** based on thedihydrobenzo[*f*]thiochromen core was the most potent one (IC_{50} = 16 nM). The *in vivo* OGTT study showed that 5 mg/kg **41d-1** displayed a moderate efficacy in improving the glucose clearance capacity (reduction percentage of $AUC_{0-120min}$: 4.38%) in ICR mice. The SAR explored will be beneficial for guiding future optimization of more potent DPP-4 inhibitors based on the three new starting points.

Experimental

Chemistry

The reagents used in the experiments were all commercially available, most of which were purchased from Energy Chemical Company. All the reactions were monitored by TLC. ^{1}H and ^{13}C spectra were recorded on a Bruker Avance-400 or Ascend 600 spectrometer in $CDCl_3$ or DMSO-d_6 with TMS as an internal standard. High-resolution mass spectra (HRMS) were acquired with a Xevo G2 TOF MS spectrometer in positive ESI mode or GCT Premier spectrometer in EI mode. Mass spectra for all intermediates were recorded on an Agilent Technologies 6100 Series Single Quadrupole LC/MS or Micromass GCT CA 055 instrument. Melting points (m.p.) were measured on a WRS-1B digital melting point apparatus. The purity of all the tested compounds was performed on an Agilent 1100 series HPLC using an Agilent XDB 5 μ C18 column (4.6 mm × 150 mm). Elution was carried out using water as mobile phase A and acetonitrile as

mobile phase B. Elution conditions were at 0 min, phase A 20% + phase B 80%; at 25 min, phase A 20% + phase B 80%. The flow rate of the mobile phase was 0.5 mL/min and the injection volume of the sample was 5 μL. The determined wavelength was 254 nm. The purity of all compounds was ≥95% as determined by HPLC analysis. The microwave reactions were executed in a microwave reactor (CEM, DISCOVERY).

Detailed synthetic procedures and spectral data for the final compounds were given in the Supporting Information. The key compound data were described as below.

trans-7-carbonitrile-2-(2,4,5-trifluorophenyl)-3,4-dihydro-2*H*-benzo[*f*]thiochromene-3-amino (41d-1). White solid. Yield: 8.0%. Mp: 120.4-120.6 °C, ^{1}H NMR (400 MHz, DMSO-d_6) δ 8.52 (s, 1H), 8.08 (d, *J* = 8.8 Hz, 1H), 7.85 (d, *J* = 8.8 Hz, 2H), 7.73-7.55 (m, 2H), 7.39 (d, *J* = 8.4 Hz, 1H), 4.62 (d, *J* = 9.2 Hz, 1H), 3.74-3.63 (m, 1H), 3.55 (dd, *J* = 17.4, 4.4 Hz, 1H), 3.06 (dd, *J* = 17.2, 9.6 Hz, 1H). ^{13}C NMR (100 MHz, DMSO-*d6*) δ 156.43 (d, *J* = 243.1 Hz), 149.26 (d, *J* = 247.8 Hz), 146.88 (d, *J* = 237.9 Hz), 135.17, 134.58, 133.96, 130.43, 130.11, 128.08, 127.56, 126.22, 123.95, 123.12, 119.63, 118.47, 107.52, 106.78, 49.79, 43.70, 33.75. HRMS (ESI): calcd for $C_{20}H_{13}F_3N_2S$ $[M+H]^+$ 371.0752, found 371.0828. Purity: 99.23% (t_R 10.97 min).

Enzyme Assays

The DPP-4 activity was determined by measuring the rate of hydrolysis of a substrate Ala-Pro-AMC (sigma), and the hydrolyzed fluorescent product amidomethylcoumarin (AMC) was continuously monitored using an excitation wavelength of 360 nm and an emission wavelength of 460 nm every 60 s for 30 min using a BioTek microplate reader. A typical reaction contained 15 ng/mL enzyme, 150 μM Ala-Pro-AMC, different concentrations of the test compounds, and assay buffer (25 mM HEPES, pH 7.5, 150 mM NaCl, 0.12 mg/mL BSA) in a total reaction volume of 100 μL. The high-throughput screening of the DPP-4 inhibitors was carried out in triplicate. And the IC_{50} data were calculated using the software Graphpad Prism 4.

Supporting Information

The supporting information for this article is available on the WWW under https://doi.org/10.1002/cjoc.2018xxxxx.

Acknowledgement (optional)

This work was supported by the National Key Research and Development Program [2016YFA0502304 to H.L.]; the National Natural Science Foundation of China (grant 81825020 to H.L., 81803437 to S.L.); the National Science & Technology Major Project "Key New Drug Creation and Manufacturing Program", China (Number: 2018ZX09711002); the Fundamental Research Funds for the Central Universities, Special Program for Applied Research on Super Computation of the NSFC-Guangdong Joint Fund (the second phase) under Grant No.U1501501. Shiliang Li is sponsored by Shanghai Sailing Program (No. 18YF1405100). Honglin Li is also sponsored by National Program for Special Supports of Eminent Professionals and National Program for Support of Top-notch Young Professionals.

References

[1] IDF Diabetes Atlas. http://www.idf.org/diabetesatlas. (accessed Nov 15, 2019)

[2] Chatterjee, S.; Khunti, K.; Davies, M. J., Type 2 diabetes. *The Lancet.* **2017**, *389* (10085), 2239-2251.

[3] Cavender, M. A.; Steg, P. G.; Smith, S. C., Jr.; Eagle, K.; Ohman, E. M.; Goto, S.; Kuder, J.; Im, K.; Wilson, P. W.; Bhatt, D. L.; Investigators, R. R., Impact of Diabetes Mellitus on Hospitalization for Heart Failure, Cardiovascular Events, and Death: Outcomes at 4 Years From the Reduction of Atherothrombosis for Continued Health (REACH) Registry. *Circulation.* **2015**, *132* (10), 923-931.

[4] Hu, C.; Jia, W., Therapeutic medications against diabetes: What we have and what we expect. *Adv. Drug Del. Rev.* **2019**, *139*, 3-15.

[5] Proenca, C.; Freitas, M.; Ribeiro, D.; Tome, S. M.; Araujo, A. N.; Silva, A. M. S.; Fernandes, P. A.; Fernandes, E., The dipeptidyl peptidase-4 inhibitory effect of flavonoids is hindered in protein rich environments. *Food Funct.* **2019**, *10* (9), 5718-5731.

[6] Waldrop, G.; Zhong, J.; Peters, M.; Rajagopalan, S., Incretin-Based Therapy for Diabetes: What a Cardiologist Needs to Know. *J. Am. Coll. Cardiol.* **2016**, *67* (12), 1488-1496.

[7] Baggio, L. L.; Drucker, D. J., Biology of incretins: GLP-1 and GIP. *Gastroenterology* **2007**, *132* (6), 2131-2157.

[8] Patel, B. D.; Ghate, M. D., Recent approaches to medicinal chemistry and therapeutic potential of dipeptidyl peptidase-4 (DPP-4) inhibitors. *Eur. J. Med. Chem.* **2014**, *74*, 574-605.

[9] Zhong, J.; Gong, Q.; Goud, A.; Srinivasamaharaj, S.; Rajagopalan, S., Recent Advances in Dipeptidyl-Peptidase-4 Inhibition Therapy: Lessons from the Bench and Clinical Trials. *Journal of diabetes research* **2015**, *2015*, 606031.

[10] Almagthali, A. G.; Alkhaldi, E. H.; Alzahrani, A. S.; Alghamdi, A. K.; Alghamdi, W. Y.; Kabel, A. M., Dipeptidyl peptidase-4 inhibitors: Anti-diabetic drugs with potential effects on cancer. *Diabetes Metab. Syndr.* **2019**, *13* (1), 36-39.

[11] Li, S.; Xu, H.; Cui, S.; Wu, F.; Zhang, Y.; Su, M.; Gong, Y.; Qiu, S.; Jiao, Q.; Qin, C.; Shan, J.; Zhang, M.; Wang, J.; Yin, Q.; Xu, M.; Liu, X.; Wang, R.; Zhu, L.; Li, J.; Xu, Y.; Jiang, H.; Zhao, Z.; Li, J.; Li, H., Discovery and Rational Design of Natural-Product-Derived 2-Phenyl-3,4-dihydro-2H-benzo f chromen-3-amine Analogs as Novel and Potent Dipeptidyl Peptidase 4 (DPP-4) Inhibitors for the Treatment of Type 2 Diabetes. *J. Med. Chem.*

2016, *59* (14), 6772-6790.

[12] Li, S.; Qin, C.; Cui, S.; Xu, H.; Wu, F.; Wang, J.; Su, M.; Fang, X.; Li, D.; Jiao, Q., Discovery of a natural-product-derived preclinical candidate for once-weekly treatment of type 2 diabetes. *J. Med. Chem.* **2019**, *62* (5), 2348-2361.

[13] Biftu, T.; Sinha-Roy, R.; Chen, P.; Qian, X.; Feng, D.; Kuethe, J. T.; Scapin, G.; Gao, Y. D.; Yan, Y.; Krueger, D.; Bak, A.; Eiermann, G.; He, J.; Cox, J.; Hicks, J.; Lyons, K.; He, H.; Salituro, G.; Tong, S.; Patel, S.; Doss, G.; Petrov, A.; Wu, J.; Xu, S. S.; Sewall, C.; Zhang, X.; Zhang, B.; Thornberry, N. A.; Weber, A. E., Omarigliptin (MK-3102): A Novel Long-Acting DPP-4 Inhibitor for Once-Weekly Treatment of Type 2 Diabetes. *J. Med. Chem.* **2014,** *57* (8), 3205-3212.

[14] Moseley, J. D.; Sankey, R. F.; Tang, O. N.; Gilday, J. P., The Newman–Kwart rearrangement re-evaluated by microwave synthesis. *Tetrahedron* **2006**, *62* (19), 4685-4689.

(The following will be filled in by the editorial staff)
Manuscript received: XXXX, 2019
Manuscript revised: XXXX, 2019
Manuscript accepted: XXXX, 2019
Accepted manuscript online: XXXX, 2019
Version of record online: XXXX, 2019

Entry for the Table of Contents

xxx

Design, Synthesis and SAR Studies of Novel and Potent Dipeptidyl Peptidase 4 Inhibitors

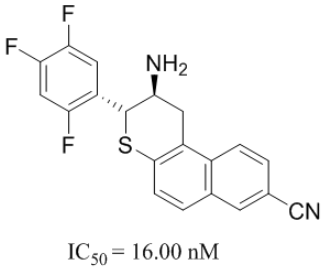

IC_{50} = 16.00 nM

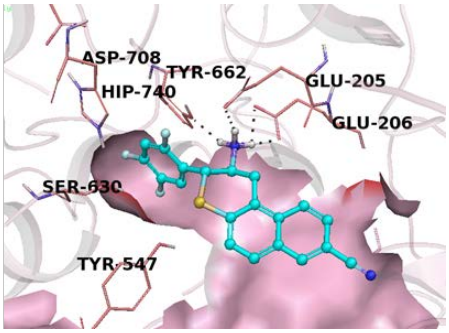

A novel DPP-4 inhibitor **41d-1** based on the scaffold of dihydrobenzo[*f*]thiochromen amine with an IC_{50} value of 16.00 nM.

Author, Corresponding Author,* Author